International Journal of Engineering Research in Electronics and Communication Engineering (IJERECE) Vol 2, Issue 6, June 2015

IRIS Recognition System Using Geodesic Active Contours for Non-Ideal IRIS Images

[1]Rapaka Satish, [2]Dr. P. Rajesh Kumar,[3]Praneeth Inteti
[1]Assistant Professor, Dept of ECE, Sir C.R.Reddy College of Engineering , Eluru, AP, India.
[2]Professor, Dept of ECE, Andhra University College of Engineering, Visakhapatnam,AP,India.
[3]PG Scholar, Dept of ECE, Sir C.R.Reddy College of Engineering , Eluru, AP, India
[1]rsatishus@rediffmail.com,[2]rajeshauce@gmail.com,[3]praneethinteti@gmail.com.

Abstract – **The stable unique epigenetic pattern of the iris make it a robust biometric trait for personal identification. The first stage of iris recognition is to isolate the actual iris region in a digital eye image. The segmentation stage is critical to the success of an iris recognition system, since data that is falsely represented as iris pattern data will corrupt the biometric templates generated, resulting in poor recognition rates. Most segmentation models in the literature assume that the pupillary, limbic, and eyelid boundaries are circular or elliptical in shape. Hence, they focus on determining model parameters that best fit these hypotheses. However, it is difficult to segment iris images acquired under non ideal conditions using such conic models. In this paper we use Geodesic Active Contours (GAC) for segmenting iris from the surrounding structures. Since active contours can 1) assumes any shape and 2) segment multiple objects simultaneously. Experimental Results on the UBIRIS and CASIA v4.0 iris databases indicate the efficacy of the proposed technique**

Keywords: Iris recognition, Iris segmentation, Feature extraction, Gabor filters, GAC, FAR, GAR

I. INTRODUCTION

A good biometric is characterized by use of a feature that is highly unique – so that the chance of any t wo people having the same characteristic will be minimal, stable – so that the feature does not change over time[1], and be easily captured – in order to provide convenience to the u ser, and prevent misrepresentation of the feature. The iris is an externally visible, yet protected organ whose unique epigenetic pattern remains stable throughout adult life. These characteristics make it very attractive for using it as a biometric for identifying individuals. Image processing techniques can be employed to extract the unique iris pattern from a digitized image of the eye, and encode it into a biometric template, which can be stored in a database. The iris is a thin circular diaphragm, which lies between the cornea and the lens of the human eye. A front-on view of the iris is shown in Figure (1). The iris is perforated close to its centre by a circular aperture known as the pupil

The function of the iris is to control the amount of light entering through the pupil. The function of an iris recognition system is to extract, represent and compare the textural intricacy present on the surface of the iris.

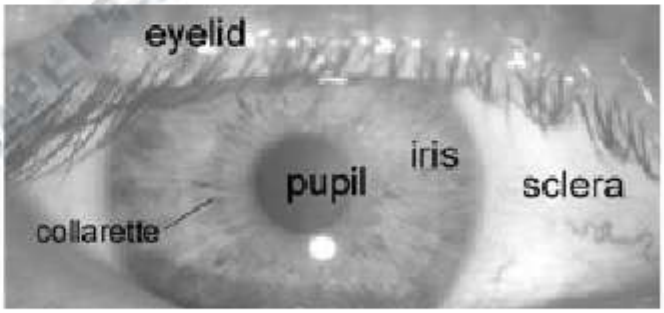

Fig1. General view of iris

It involves segmentation, enhancement, feature extraction and feature matching.

In this paper, Geodesic Active Contour (GAC) models are used to accurately localize the structure of the iris present in an image of the eye. The use of a GAC model obviates the fitting of a tight boundary around the iris. The remainder of the paper is organized as follows. Segmentation and encoding methods are first described and later a brief overview of segmentation by using geodesic active counters, experimental results and lastly the paper is concluded.

II. SEGMENTATION AND ENCODING METHODS

Segmentation is the process of dividing an image into its constituent parts. Process of segmenting an iris can be carried out in various methods such as Daugman's algorithm using Integro Differential Operator [2],[3], Masek's[4] method using Circular Hough Transform.

2.1 Daugman's algorithm for iris segmentation

Daugman [2], [3] uses a texture-based method to encode irides. Integro differential operator act as circular edge detector and have been used to determine the inner and the outer boundaries of the iris. They also have been used to determine the elliptical boundaries of the lower and the upper eyelids. An integro differential operator can be defined as,

$$\max_{(r,x_0,y_0)} \left| \frac{\partial}{\partial r} G_\sigma(r) * \oint_{r,x_0,y_0} \frac{I(x,y)}{2\pi r} ds \right|$$

(1)

Where I(x, y) is the image, r is the radius of the pupil or iris, (x0, y0) its center and G□ □r□ is the Gaussian smoothing function with scale □ . Thus, the integro differential operator searches for a maximum partial derivative of the image over a circular boundary by varying the radius r and center (x0, y0). The eyelids can be detected in a similar fashion by performing the integration over an elliptical boundary rather than a circular one. The output of the segmentation process is a binary mask that indicates the iris and non-iris pixels in the image.

2.2 Circular Hough Transform for iris segmentation

The Masek's[4] system performs its contour fitting in two steps. First, the image intensity information is converted into a binary edge-map. Second, the edge points vote to instantiate particular contour parameter values. The edge map is recovered via gradient-based edge detection. This operation consists of thresholding the magnitude of the image intensity gradient,

$$\left| \nabla G(x,y) * I(x,y) \right|$$

$$\text{Where } G(x,y) = \frac{1}{2\pi\sigma^2} e^{-\frac{(x-x_c)^2+(y-y_c)^2}{2\sigma^2}}$$

is a two-dimensional Gaussian with center (xo , yo) and standard deviation □ that smooths the image to select the spatial scale of edges under consideration. In order to incorporate directional tuning, the image intensity derivatives are weighted to favor certain ranges of orientation prior to taking the magnitude. For example, prior to contributing to the fit of the limbic boundary contour, the derivatives are weighted to be selective for vertical edges. The voting procedure is realized via Hough transforms on parametric definitions of the iris boundary contours. In particular, for the circular limbic or pupillary boundaries and a set of recovered (x j , y j) , j = 1 , 2 , 3 , … ,

$$h(x_j, y_j, x_c, y_c, r) = \begin{cases} 1, & \text{if } g(x_j, y_j, x_c, y_c, r) = 0 \\ 0, & \text{otherwise} \end{cases} \quad (3)$$

With

$$g(x_j, y_j, x_c, y_c, r) = (x_j - x_c)^2 + (y_j - y_c)^2 - r^2$$

For each edge point for every parameter triple that represents a circle through that point. Correspondingly, the parameter triple that maximizes H is common to the largest number of edge points and is a reasonable choice to represent the contour of interest. In implementation, the maximizing parameter set is computed by building H (xc , y c , r) as an array that is indexed by discretized values for xc , yc and r . Once populated, the array is scanned for the triple that defines its largest value. Contours for the upper and lower eyelids are fit in a similar fashion using parameterized g (x j , y j , xc , y c , r) parabolic arcs in place of the circle parameterization. Just as the Daugman system relies on standard techniques for iris localization, edge detection followed by a Hough transform is a standard machine vision technique for fitting simple contour models to images

2.3 2D Gabor Filters for feature extraction

Gabor filters are used to encode the normalized image that is obtained from the daugman's rubber sheet model. Gabor filters are clearly explained as follows. Gabor filters are able to provide optimum conjoint representation of a signal in space and spatial frequency. A Gabor filter is constructed by modulating a sine/cosine wave by a Gaussian. This is able to provide the optimum conjoint localization in both space and frequency, since a sine wave is perfectly localized in frequency, but not localized in space. Modulation of the sine with a Gaussian provides localization in The centre frequency of the filter is specified by the frequency of the sine/cosine wave, and the bandwidth of the filter is specified by the width of the Gaussian. Daugman makes uses of a 2D version of Gabor filters in order to encode iris pattern data. A 2D Gabor filter over an image domain (x,y) is represented as.

$$G(x,y) = e^{-\pi[(x-x_0)^2/\alpha^2 + (y-y_0)^2/\beta^2]} e^{-2\pi i[u_0(x-x_0)+v_0(y-y_0)]} \quad (4)$$

Where (x0,y0) specify position in the image, (α,β) specify the effective width and length, and (u0,v0) specify modulation, which has spatial frequency and orientation respectively are

$$\omega_0 = \sqrt{u_0^2 + v_0^2} \text{ and } \theta = \arctan(v_0 / u_0)$$

Daugman demodulates the output of the Gabor filters in order

to compress the data. This is done by quantizing the phase information into four levels, for each possible quadrant in the complex plane. Only phase information is used for recognizing irises because amplitude information is not very discriminating, and it depends upon extraneous factors such as imaging contrast, illumination, and camera gain [2]. Taking only the phase will allow encoding of discriminating information in the iris, while discarding redundant information such as illumination, which is represented by the amplitude component. These four levels are represented using two bits of data, so each pixel in the normalized iris pattern corresponds to two bits of data in the iris template. A total of 2,048 bits are calculated for the template, and an equal number of masking bits are generated in order to mask out corrupted regions within the iris. This creates a compact 256-byte template, which allows for efficient storage and comparison of irises. The Daugman system makes use of polar coordinates for normalization, therefore in polar form the filters are given as

$$H(r,\theta) = e^{-\pi(\alpha-\phi)^2} e^{-(r-r_0)^2} e^{-i(\omega(\theta-\theta_0))} \quad (5)$$

Where(α,β) are the same as in the above equation and (r 0 , θ 0) specify the centre frequency of the filter.Thedemodulation and phase Quantization process can be represented as

$$\int\int I(\rho,\varphi) e^{-i\omega(\theta_0-\varphi)} e^{-(r_0-\rho)^2/\alpha^2} e^{-(\theta_0-\varphi)^2/\beta^2} \rho\, d\rho\, d\varphi \quad (6)$$

where h{Re, Im} can be regarded as a complex valued bit whose real and imaginary components are dependent on the sign of the 2D integral, and I(ρ,φ) is the raw iris image in a dimensionless polar coordinate system. Gabor encoding gives two outputs. They are iris template and iris mask as shown Fig2. Iris template contains the information of iris and iris mask represents the valid portion that is to be compared in finding hamming distance

Fig2(a): Encoded iris template

Fig2(b): Iris mask

III. SEGMENTATION BY USING GEODESIC ACTIVE COUNTERS

The iris localization procedure can be broadly divided into two stages namely Pupil segmentation and Iris segmentation.

3.1 Pupil Segmentation

To detect the pupillary boundary, the eye image is first smoothed using a 2-D median filter[5] and the minimum pixel value is determined. The iris is then binarized using a threshold value (M). As expected, apart from the pupil, other dark regions of the eye (e.g., eyelashes) fall below this threshold value 25+M. A 2-D median filter is then applied on the binary image to discard the relatively smaller regions associated with the eyelashes. This reduces the number of candidate iris pixels detected as a consequence of thresholding. Based on the median-filtered binary image, the exterior boundaries of all the remaining objects are traced. Generally the largest boundary of the remaining regions of the eye corresponds to the pupil. However, when the pupil is constricted, it is very likely that the boundary of the detected region corresponding to the eyelashes is larger than that of the pupil. So a circle-fitting procedure is executed on all detected regions. The equation of a circle is given by,

$$x^2 + y^2 + a_1 x + a_2 y + a_3 = 0 \quad (7)$$

where (x,y) represent the co-ordinates of a point on the circle. The coordinates of the centre is given in equation (8).

$$x_0 = -\frac{a_1}{2}; y_0 = -\frac{a_2}{2} \quad (8)$$

Finally, the circle whose circumference contains the maximum number of black pixels is deemed to be the detected pupil. Regions with diameters more than half the image size are not considered. Figure3 shows an iris image containing dark eyelashes and the correctly segmented pupil using the aforementioned algorithm. Sometimes, specular reflections can occur near the boundary of the pupil that may confound the pupil segmentation procedure. Hence, if specular reflection (bright spots in an image) is detected in the vicinity of the pupil, it is "inpainted" using the surrounding in-f ormation. Inpainting is a process to fill in the missing portions of an image (in our case specular -reflections) to improve its integrity. Figure demonstrates that the pupil detection procedure is made more robust by Inpainting those specular reflections in the iris image that occur near the pupil boundary. Since the specular reflections are detected by a simple image thresholding technique, other regions of the eye that are over-exposed to light may also be incorrectly detected.

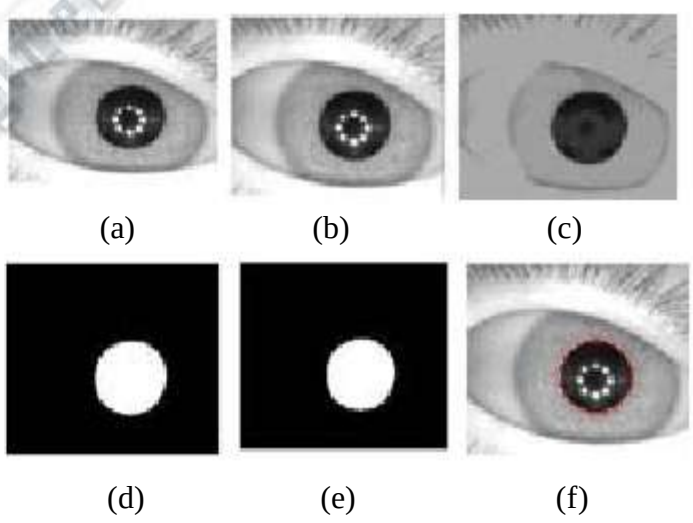

Fig3. (a) Iris image , (b) Smoothed image, (c) Inpainted Image,(d) Thresholded image, (e) Median filtered image,
(f) Pupil segmented image.

3.2 Iris Segmentation

To detect the limbic boundary of the iris, a novel scheme based on a level sets representation of the GAC model[5] is employed. This approach is based on the relation between active contours and the computation of geodesics (minimal length curves)[6]. The technique is to evolve the contour from inside the iris under the influence of geometric measures of the iris image. GACs combine the energy minimization approach of the classical "snakes" and the geometric active contours based on curve evolution. The proposed technique is significantly different from the one proposed by Daugman. The active contour is defined as a Fourier boundary approximated using the coefficients of the Fourier series. The technique relies on the order of the Fourier series to approximate the inner and outer boundaries of the iris.

GAC's: Let $\gamma(t)$ be the curve that has to gravitate toward the boundary of any object, at a particular time as shown in Fig. 4. The time corresponds to the iteration number. Let ψ be a function defined as a signed distance function from the curve $\gamma(t)$. Thus, $\psi(x,y)$ distance of point (x,y) to the curve $\gamma(t)$.

$$\psi(x,y) = \begin{cases} 0 & \text{if } (x,y) \text{ is on the curve} \\ < 0 & \text{if } (x,y) \text{ is inside the curve} \\ > 0 & \text{if } (x,y) \text{ is outside the curve} \end{cases} \quad (9)$$

ψ is of the same dimension as that of the image I(x,y) that is to be segmented. The curve $\gamma(t)$ is a level set of the function, ψ. Level sets are the set of all points in ψ where some constant. Thus, $\psi = 0$ is the zeroth level set, $\psi = 1$ is the first level set and so on. ψ is the implicit representation of the curve $\gamma(t)$ and is called as the embedding function since it embeds the evolution of $\gamma(t)$. The embedding function evolves under the influence of image gradients and regions characteristics so that the curve $\gamma(t)$ approaches the boundary of the object. Thus, instead of evolving the parametric curve $\gamma(t)$ Lagrangian approach used in snakes)[7],[8], the embedding function itself is evolved. In our algorithm, the initial curve $\gamma(t)$ is assumed to be a circle of radius just beyond the papillary boundary. Let the curve $\gamma(t)$ be the zeroth-level set of the embedding function. This implies that

$\gamma(t)$

is assumed to be a circle of radius just beyond the papillary boundary. Let the curve $\gamma(t)$ be the zeroth-level set of the embedding function. This implies that

$$\frac{d\psi}{dt} = 0 \quad (10)$$

By chain rule,

$$\frac{d\psi}{dt} = \frac{\partial\psi}{\partial x}\frac{dx}{dt} + \frac{\partial\psi}{\partial y}\frac{dy}{dt} + \frac{\partial\psi}{\partial t}$$

i.e.,

$$\frac{\partial\psi}{\partial t} = -\nabla\psi \cdot \gamma'(t)$$

Splitting the $\gamma(t)$ in the normal N(t) and tangential T(t) directions,

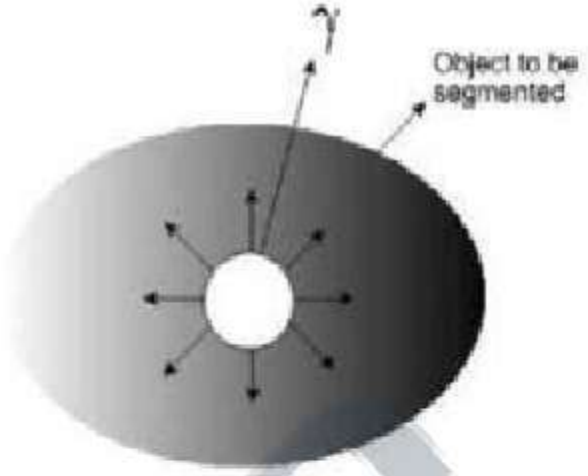

Fig4.Evolution curve

$$\frac{\partial\psi}{\partial t} = -\nabla\psi \cdot \left(v_N N(t) + v_T T(t)\right) \quad (11)$$

Now, since $\nabla\psi$ is perpendicular to the tangent to $\gamma(t)$

$$\frac{\partial\psi}{\partial t} = -\nabla\psi \cdot \left(v_N N(t)\right) \quad (12)$$

The normal component is given by

$$N = \frac{\nabla\psi}{\nabla\psi} \quad (13)$$

Substituting this in (12)

$$\frac{\partial\psi}{\partial t} = -v_N \nabla\psi \quad (14)$$

Let vN be a function of the curvature of the curve γ, stopping function (to stop the evolution of the curve) and the inflation force c (to evolve the curve in the outward direction) such that,

$$\frac{\partial\psi}{\partial t} = -\alpha\kappa\frac{\nabla\psi}{\nabla\psi} + c\kappa_s\nabla\psi \quad (15)$$

Thus, the evolution equation for ψ_t such that $\psi(t)$ remains
the zeroth level set is given by

$$\psi_t = -K\left(c + \epsilon\kappa\right)\left|\nabla\psi\right| + \nabla\psi \cdot \nabla K \quad (16)$$

Where K , the stopping term for the evolution, is an image dependant force and is used to decelerate the evolution near the boundaries; C is the velocity of the evolution;ε indicates the degree of smoothness of the level sets; and is the curvature of the level sets computed as

$$K=\frac{\psi_{xx}\psi_{y}^{2}-2\psi_{x}\psi_{y}\psi_{xy}+\psi_{yy}\psi_{x}^{2}}{\left(\psi_{x}^{2}+\psi_{y}^{2}\right)^{3/2}} \quad (17)$$

where ψ_x is the gradient of the image in the x-direction; ψ_y is the gradient in the direction; ψ_{xx} is the second-order gradient in the x-direction; ψ_{yy} is the second-order gradient in the y-direction; and ψ_{xy} is the second-order gradient, first in the x-direction and then in the y-direction. Equation(16) is the level set representation of the GAC model. This means that the level-set C of _ is evolving according to

$$C_t = K\left(c+\in\kappa\right)N-\left(\nabla K.N\right)N \quad (18)$$

Where N is the normal to the curve. The first term(κ. N) provides the smoothing constraints on the level sets by reducing the total curvature of the level sets. The second term (cN) acts like a balloon force[9] and it pushes the curve outward towards the object boundary. The goal of the stopping function is to slow down the evolution when it reaches the boundaries. However, the evolution of the curve will terminate only when K=0, i.e., near an ideal edge. In most images, the gradient values will be different along the edge, thus, necessitating different K values. In order to circumvent this issue, the third geodesic term(∇K . N) is necessary so that the curve is attracted toward the boundaries (∇_ points toward the middle of the boundary). This term makes it possible to terminate the evolution process even if (a) the stopping function has different values along the edges, and (b) gaps are present in the stopping function.

The stopping term used for the evolution of level sets is given

$$K(x,y)=\frac{1}{1+\frac{\nabla G(x,y)*I(x,y)}{k}^{\alpha}} \quad (19)$$

where I(x,y) is the image to be segmented, and k and _ are constants. As can be seen, this term K(x,y) is not a function of t. Consider an iris image to be segmented as shown in Fig 5(a). The stopping function K obtained from this image is shown in Fig5(b). (In our implementation k=2.8 and α=8.

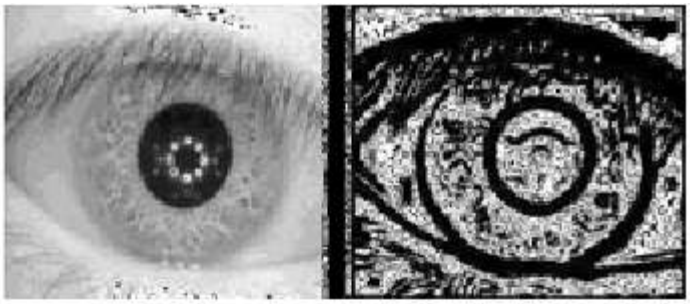

(a) (b)

Fig5: (a) Image to be segmented (b) The stopping function.

Let the radii of the pupil is R, then a contour is first initialized at a radii R+10 from the center of the pupil. The embedding function ψ is initialized as a signed distance function to γ(t=0) . Discretizing eq(16)

$$[\psi_{i,j}^{t+1}-\psi_{i,j}^{t}]/\Delta t=-cK_{i,j}\nabla\psi^{+}-K_{i,j}(c+\varepsilon\kappa_{i,j})\nabla\psi^{+})+\nabla\psi_{i,j}\nabla K_{i,j}$$

(20) After evolving the embedding function □ according to eq(20) The curve starts to grow until it satisfies the stopping criterion defined by the stopping function K. fig(6) shows an image to be segmented and segmented image. But at times, the contour continues to evolve in a local region of the iris where the stopping criterion is not strong. This leads to over evolution of the con-tour. To avoid it, we minimize the Thin Plate Spline energy of the contours. Thin Plate Spline is an interpolation method that finds the minimal "bendin g energy" to pass a smooth surface though a set of given points. The name "Thin Plate Splines" can be thought of as a si mulation of how a thin metal plate would bend if it was forced through some fixed control points. Thus, the thin plate spline energy to pass a smooth surface though coplanar points will be zero where as if the points are nonplanar, the thin plate spline energy will increase with the distance be-tween these points. In this work, Thin Plate Splines are used for minimizing the energy of the contour so as to prevent the contour from evolving in a highly non-uniform manner. Here, the evolving contour can be thought of as the smooth surface which needs to be fitted through the points on the iris boundary. Thus, if all points on the contour lie on a circle, then the thin plate spline energy will be zero; however, if the contour starts evolving non-uniformly, the thin plate spline energy to fit the contour through these points will start increasing. By computing the difference in energy between two successive contours, the evolution scheme can be regulated. If the difference between the contours is less than a threshold (indicating that the contour evolution has stopped at most places), then the contour evolution process is stopped. In our implementation, this threshold is set to 1.If the Thin Plate Spline energy of the level sets is not minimized, the contour might continue evolving if the stopping function does not have a high magnitude. Minimizing the thin plate spline energy of level sets yields a more precise contour of the iris boundary. One important feature of GACs is their ability to handle "splitti ng and merging"boundaries. This is especially important in the case of iris segmentation since the radial fibres maybe thick in some portions of the iris, or the crypts present in the ciliary region may be unusually dark, leading to prominent edges in the stopping function. If the segmentation technique is based on parametric curves (e.g., the snakes segmentation technique), then the evolution of the curve might terminate at these local minima. However, GACs are able to split at such local minima

and merge again. Thus, they are able to effectively deal with the problems of local minima thereby ensuring that the finalcontour corresponds to the true iris boundary.

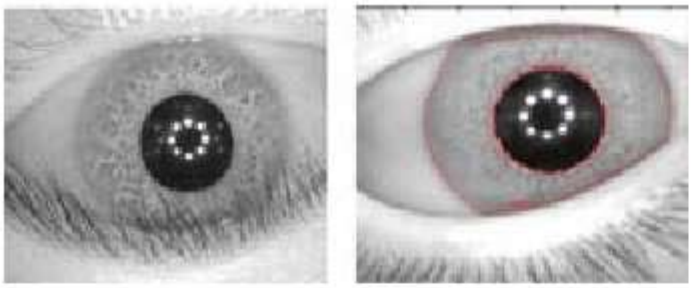

(a) (b)

Fig6.(a) Input image;(b) Segmented image

EXPERIMENTAL RESULTS

The matching performance of our segmentation algorithm was evaluated on the CASIA and UBIRIS non-ideal iris image datasets. The CASIA iris database has 756 iris images corresponding to 108 different irises (7 images per iris). Each image is of size 320×280. The UBIRIS no n-ideal iris database has the left and right irises of 207 individuals. There are between 4−15 images of both the left and right irises of each individual. The total number of images in the UBIRIS non-ideal iris database is 2,678. Each image is of size 200×150. Three techniques, viz., GACs, Daugman's an d Masek's segmentation technique were used to segment the iris. The encoding and normalization of the iris was then carried From the ROC curves for the CASIA database (Figure6), it is clear that the matching performance of the iris recognition system significantly improves when geodesic active contour is used for segmentation. For example, the GAR (GenuineAcceptance Rate), at a fixed FAR (False Acceptance Rate) of 0.01% is (a) 94% using geodesic active contours for segmentation; (b) 91.5% using Masek's code; and (c)88% using integro-differential operators.

Upon analyzing the performance, it was found that many irises in the CASIA database were severely occluded by the presence of eyelids and eyelashes. Thus the irises, which are occluded to a large extent, do not have sufficient iris information. The figure also shows the performance of the iris recognition system when such irises are rejected by the System.

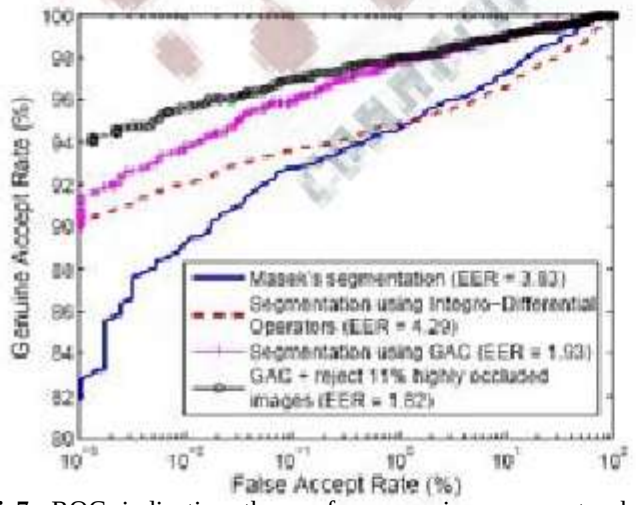

Fig7. ROC indicating the performance improvement when CASIA iris images with very large occlusion are rejected.

IMAGE 1

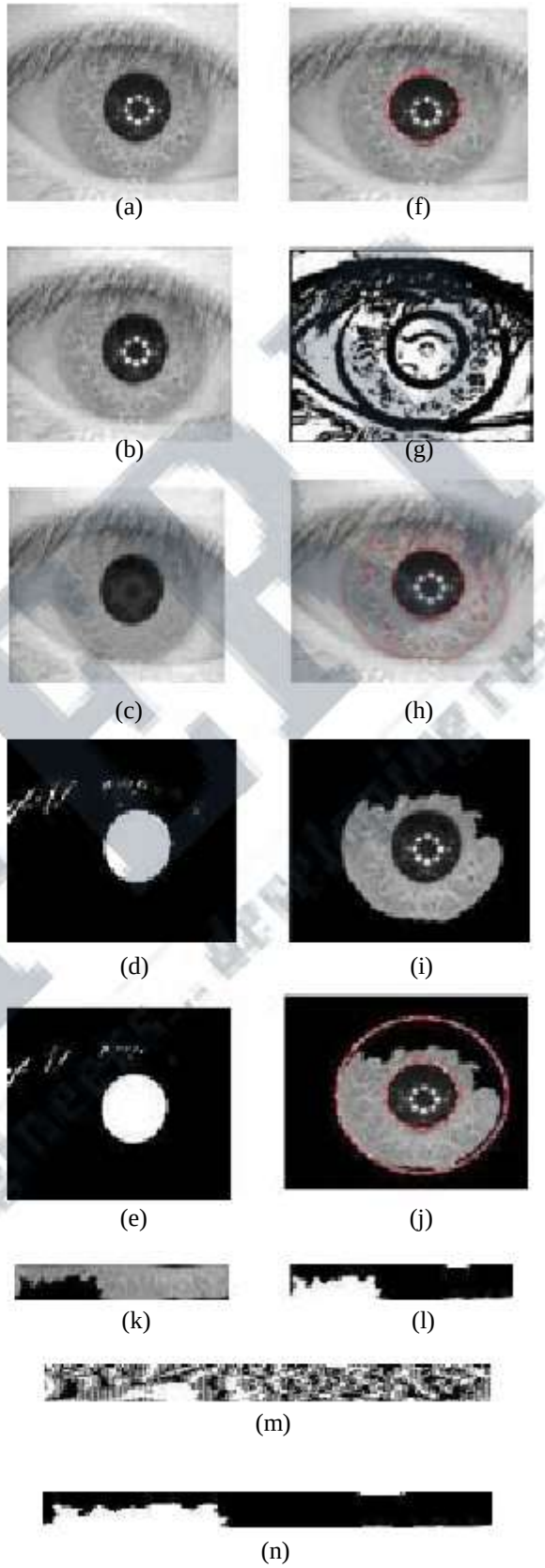

Fig8: (a)Original image,(b)smoothed image,(c)inpainted image,(d) Thresholded image, (e)median filtered image, (f) pupil- segmented image,(g) Boundary attractor(h) segmented - output,(i)masked image,(j)normalization ring,(k)normalized image,(l)noise array, (m)iris template,(n)iris mask.

IMAGE 2

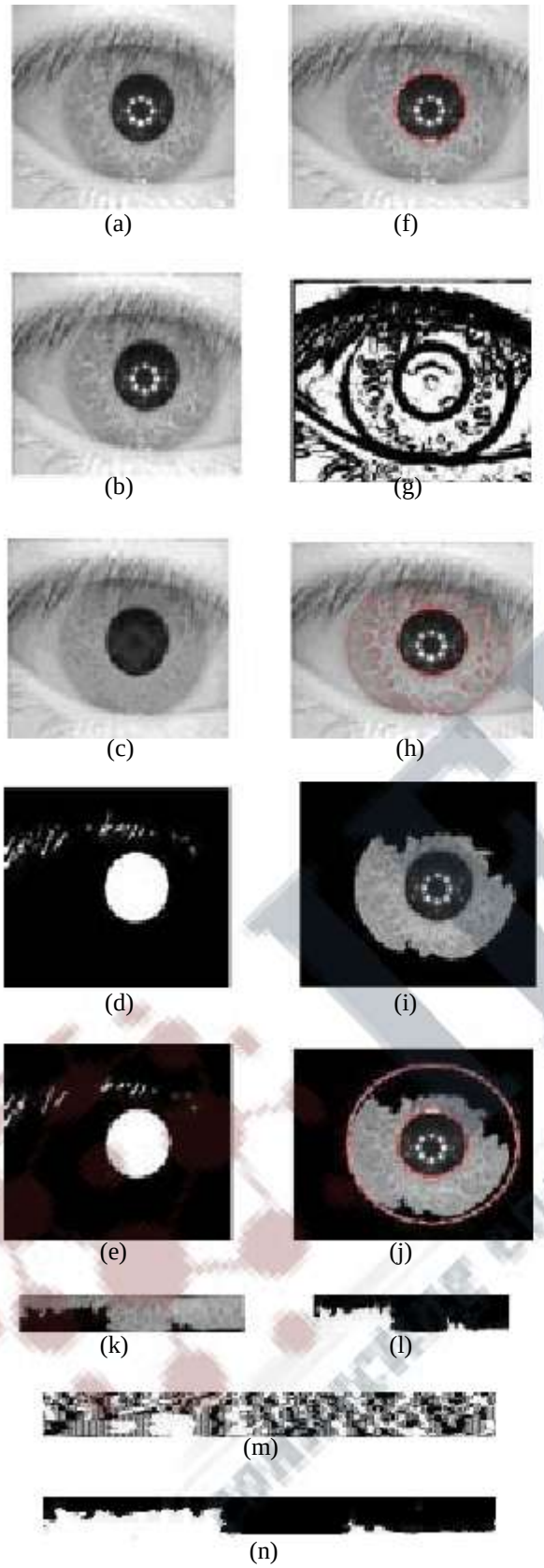

Fig9: (a)Original image,(b)smoothed image,(c)inpainted image,(d) Thresholded image, (e)median filtered image, (f) pupil- segmented image,(g) Boundary attractor(h) segmented output,(i)masked image,(j)normalization ring,(k)normalized image,(l)noise array, (m)iris template,(n)iris mask.

SUMMARY AND FUTURE WORK

Here segmentation is done on images having different features. Eye lashes are eliminated and useful portion of iris was extracted with high accuracy. Iris localization is done by geodesic active contours. Hamming distance represents the matching criteria of two iris patterns. It gives the Ratio of agreed (matched) bits to the matched bits between two iris codes. Typical roadbacks to consistent performance include limited capture range, noise sensitivity and poor convergence which can be exploited by using the vector field convolution to the geodesic active contours.

REFERENCES:

[1] F. H. Adler, Physiology of the Eye: Clinical Application (fourth edition). London: The C.V. Mosby Company, 1965.

[2] J. Daugman, “New methods in iris recognition,” IEEE Trans. Syst.,Man, Cybern., vol. 37, no. 5, pt. B, pp. 1167– 1175, 2007.

[3] J. G. Daugman, “High confidence visual recognit ion of persons by a test of statistical independence,” IEEE Trans. Pattern Anal. Mach. Intell., vol. 15, no. 11, pp. 1148–1160, Nov. 1993.

[4] Libor Masek, Peter Kovesi. MATLAB Source Code for a Biometric Identification System Based on Iris Patterns. The School of Computer Science and Software Engineering, The University of Western Australia. 2003.

[5] A. Ross and S. Shah, “Segmenting nonideal irise s using Geodesic Active Contours,” in Proc. Biometrics Symp. (BSYM), Baltimore, MD, Sep. 2006.

[6] V. Caselles, R. Kimmel, and G. Sapiro, “Geodesi c active ontours,” Int. J. Comput. Vision, vol. 22, no. 1, pp. 61–79, Feb./Mar. 1997.

[7] M. Kass, A. Witkin, and D. Terzopoulos, “Snakes : Active contour models,” Int. J. Comput. Vision, vol. 1, no. 4, pp. 321– 331, 1987.

[8] L. Zhukov, K. Museth, D. Breen, R. Whitaker, and A. Barr, “Level set modeling and segmentation of DT-MRI brai n data,” J. Electron. Imag.,vol. 12, no. 1, pp. 125–133, Jan. 2003.

[9] L. D. Cohen, “On active contour models and ball oons,” Comput. Vision,Graph., Image Process.: Image Understand., vol. 53, no. 2, pp.211–218, 1991.

[10] L. Masek and P. Kovesi, Matlab Source Code for Biometric Identification System Based on Iris Patterns The School of Comput. Sci.Software Eng., The Univ. Western Australia, 2003 [Online].
Available: http://www.csse.uwa.edu.au/~pk/studentprojects/libor/sourcec ode.html

[11] The CASIA Iris Image Database [Online]. Available: http://www.sinobiometrics.com